Development and evaluation of an automated tree detection–delineation algorithm for monitoring regenerating coniferous forests

D.A. Pouliot, D.J. King, and D.G. Pitt

Abstract: An algorithm is presented for automated detection–delineation of coniferous tree regeneration that combines strategies of several existing algorithms, including image processing to isolate conifer crowns, optimal image scale determination, initial crown detection, and crown boundary segmentation and refinement. The algorithm is evaluated using 6-cm pixel airborne imagery in operational regeneration conditions typically encountered in the boreal forest 5–10 years after harvest. Detection omission and commission errors as well as an accuracy index combining both error types were assessed on a tree by tree basis, on an aggregated basis for each study area, in relation to tree size and the amount of woody competition present. Delineation error was assessed in a similar manner using field-measured crown diameters as a reference. The individual tree detection accuracy index improved with increasing tree size and was >70% for trees larger than 30 cm crown diameter. Crown diameter absolute error measured from automated delineations was <23%. Large crown diameters tended to be slightly underestimated. The presence of overtopping woody competition had a negligible effect on detection accuracy and only reduced estimates of crown diameter slightly.

Résumé : Cet article présente un algorithme pour la détection et la délinéation automatique de la régénération de conifères. Il combine les stratégies de plusieurs algorithmes existants incluant le traitement d'image pour isoler la cime des conifères, la détermination de l'échelle optimale de l'image, la détection préliminaire de la cime et la segmentation du contour de la cime avec son raffinement. L'algorithme est évalué en utilisant l'imagerie aérienne avec des pixels de 6 cm dans des conditions opérationnelles de régénération typiquement rencontrées en forêt boréale cinq à dix ans après la récolte. Les erreurs d'omission et de commission ainsi qu'un indice de précision combinant les deux types d'erreurs ont été analysés individuellement pour chaque arbre et pour des regroupements d'arbres dans chaque aire d'étude en relation avec la taille des arbres et le nombre de compétiteurs présents. L'erreur de délinéation a été analysée de façon similaire en utilisant le diamètre des cimes mesurées sur le terrain comme référence. L'indice de précision pour la détection des individus augmente avec la taille de l'arbre et dépasse 70 % pour les arbres dont la cime a plus de 30 cm de diamètre. L'erreur absolue de délinéation automatique du diamètre de la cime est inférieure à 23 %. Les grands diamètres de cime tendent à être sous-estimés. La présence de compétiteurs qui surpassent la régénération a un effet négligeable sur la précision de détection et réduit seulement légèrement les valeurs estimées du diamètre des cimes.

[Traduit par la Rédaction]

Introduction

Sustainable forest management depends on successful regeneration of disturbed forest areas. To ensure regeneration success, forestry professionals require timely information regarding the abundance, distribution, and size of crop trees and noncrop (e.g., nonconiferous vegetation) competitors. Currently, field-based monitoring is the principal means used to collect information regarding regeneration status. Such monitoring is usually conducted by qualitative visual assessment and (or) quantitative assessment using statistically based plot sampling designs (Pitt et al. 1997). The objective of the former is to use expert knowledge in the rapid collection of a large amount of information, but the procedure is highly subjective. Plot-based assessment methods minimize subjectivity, but are highly labour intensive and costly.

Remote sensing based methods have the potential to provide the required information in a more objective manner, at lower cost, and with greater coverage than is attainable using field sampling. The application of remote sensing for regeneration assessment has, to date, largely involved manual interpretation of large-scale photography. Results have shown that useful estimates of conifer stocking, species, crown size, health condition, and stratification of key vegetation complexes can be made (Goba et al. 1982; Hall 1984; Hall and Aldred 1992; Pitt and Glover 1993; Pitt et al. 2000). However, these methods have not found widespread use because they tend to be highly specialized, time consuming, and sub-

Received 4 October 2004. Accepted 29 June 2005. Published on the NRC Research Press Web site at http://cjfr.nrc.ca on 28 October 2005.

D.A. Pouliot[1] and D.J. King. Geography and Environmental Studies, Carleton University, 1125 Colonel By Drive, Ottawa, ON K1S 5B6, Canada.
D.G. Pitt. Canadian Forest Service, Great Lakes Forestry Centre, P.O. Box 490, Sault Ste. Marie, ON P6A 5M7, Canada.

[1]Corresponding author (e-mail: darren.pouliot@ccrs.nrcan.gc.ca).

 doi: 10.1139/X05-145

jective, requiring specially trained personnel and equipment (King 2000).

Automated tree detection–delineation using high spatial resolution remotely sensed imagery provides a potentially efficient means to acquire information needed for forest regeneration management decisions. Tree detection can provide estimates of tree abundance and spatial pattern that are useful for evaluating density and stocking objectives as well as inputs for growth modeling. Delineation of individual tree crowns can potentially enhance species composition inventory through analysis of within-crown spectral data (Leckie et. al. 2003; Leckie et al. 2005), spatial data (Haddow et al. 2000; Erikson 2004), lidar data (Holmgren and Persson 2003), and crown shape (Brandtberg 1999). Recent research has also shown the potential for mapping damage due to insects and disease (Leckie et al. 2004). Further, delineated crown dimensions can be used to model tree structural variables such as height, volume, or biomass (Culvenor 2000; Hayward and Slaymaker 2001; Persson et al. 2002).

Much of the research on image-based automated tree detection–delineation has focused on mature forests for purposes of forest inventory. Techniques are varied, but generally use the same basic radiometric properties of tree crowns. These key properties are the association of the approximate crown apex with a local maximum image brightness value and decreasing brightness towards the crown edges. This radiometric crown model has been described as analogous to that of a mountainous landscape, where peaks are the highest elevation, approximately representing crown apexes, and surrounding valleys are the lower elevations, representing the space between crowns or where crowns overlap or touch. Some algorithms are explicitly linked to this concept. One of the first, developed by Gougeon (1995), incorporates a procedure to outline the local brightness "valleys" between crowns. A rule set is then applied to the valley network to refine crown boundaries and split and merge crowns. However, the majority of algorithms approach detection–delineation as two separate tasks. These methods typically apply some method of local maximum detection to first detect crowns and then use these as reference points for crown delineation. Methods applied for tree detection include (1) enhancement and thresholding (Dralle and Rudemo 1996; Walsworth and King 1999), where a global image operation such as smoothing or high-pass filtering is applied and the resulting pixel brightness values within a defined range are extracted as estimates of tree locations; (2) template matching (Pollock 1999) involving the correlation between a geometric–radiometric tree crown model and image data; (3) multiscale edge detection (Brandtberg and Walter 1998), where the occurrence of edges over several image scales is examined to define a region in which the brightest pixel value is taken as a representative location of the tree apex; (4) local maximum filtering (Pinz 1999; Culvenor 2000; Gougeon and Leckie 1999; Niemann et al. 1999; Wulder et al. 2000; Pitkanen 2001; Pouliot et al. 2002; Erikson 2003), where the maximum pixel brightness value in a moving-window sample of a specified size is taken to represent the tree apex; and (5) gradient following (Persson et al. 2002), where maxima are identified by following the local upward gradient from a given pixel to the brightest local value.

Tree delineation has been accomplished mostly through forms of (1) spatial clustering (Brandtberg and Walter 1998; Walsworth and King 1999; Erikson 2003) involving the identification of groups of pixels related by defined criteria, (2) valley detection based on local minima (Gougeon 1995; Persson et al. 2002), (3) local edge detection (Pouliot et al. 2002), and (4) a combination of valley detection and spatial clustering (Culvenor et al. 2000). A more detailed review of detection–delineation algorithms is provided in Culvenor (2003).

Each of these algorithms has been shown to provide reasonable results in the specific imaging and scene conditions used. However, the complementary benefits of these approaches have not been combined into an integrated algorithm that could be robust under a variety of operational forest conditions. In addition, very little development and evaluation has been carried out in regenerating forests, where canopies tend to range from open to closed over relatively fine spatial scales and crown sizes can be highly variable. In regenerating forests, algorithms developed by Gougeon and Leckie (1999) and Pouliot et al. (2002) have been evaluated. The results of these studies were encouraging, but both were conducted in controlled experimental study sites that were not representative of typical postdisturbance conditions that would exist after clear-cut harvesting, planting with natural ingress, or intense fire. In these conditions, tree size and spacing is considerably more variable, competing woody stems often overtop conifers, topography is wide ranging, and ground brightness is more inconsistent. Thus, it is difficult to determine whether any of the approaches would provide suitable results in more operational conditions.

This research was designed to address the issues identified previously, that is, to combine beneficial and complementary aspects of existing detection–delineation algorithms to produce a new algorithm that is robust under the diverse conditions encountered in typical conifer regeneration conditions. Specifically, the objectives of the research were to (1) develop an integrated and robust tree detection–delineation algorithm for operational regenerating coniferous forest conditions imaged with high spatial resolution imagery and (2) evaluate the algorithm accuracy and sources of error in relation to tree size and amount of woody competition.

Materials and methods

Study site

The study site consisted of three operational cutovers located northeast of Sioux Lookout, Ontario, Canada, in the Buchanan Inc. forest management unit. The three cutovers represent various regeneration conditions, most distinctly marked by differences in competing vegetation levels that reflect different soil and microclimate conditions. These sites were labeled high (50°46′N, 91°25′W), moderate (50°18′N, 91°39′W), and low (50°50′N, 91°21′W) competition (Fig. 1).

The high site was planted in 1992 with white spruce (*Picea glauca* (Moench) Voss). Species composition at the time of this study was 89% white spruce, 3% jack pine (*Pinus banksiana* Lamb.), and 8% balsam fir (*Abies balsamea* (L.) Mill.). Total conifer density was 1784 stems/ha. The average crown diameter was 77 ± 44 cm (mean ± standard deviation (SD)), ranging from 12 to 290 cm. The large crowns in the site were advanced regeneration that was present postdisturbance. The average tree height was 138 cm. The site supported a variety of herbaceous and woody noncrop vegetation spe-

Fig. 1. Study site locations.

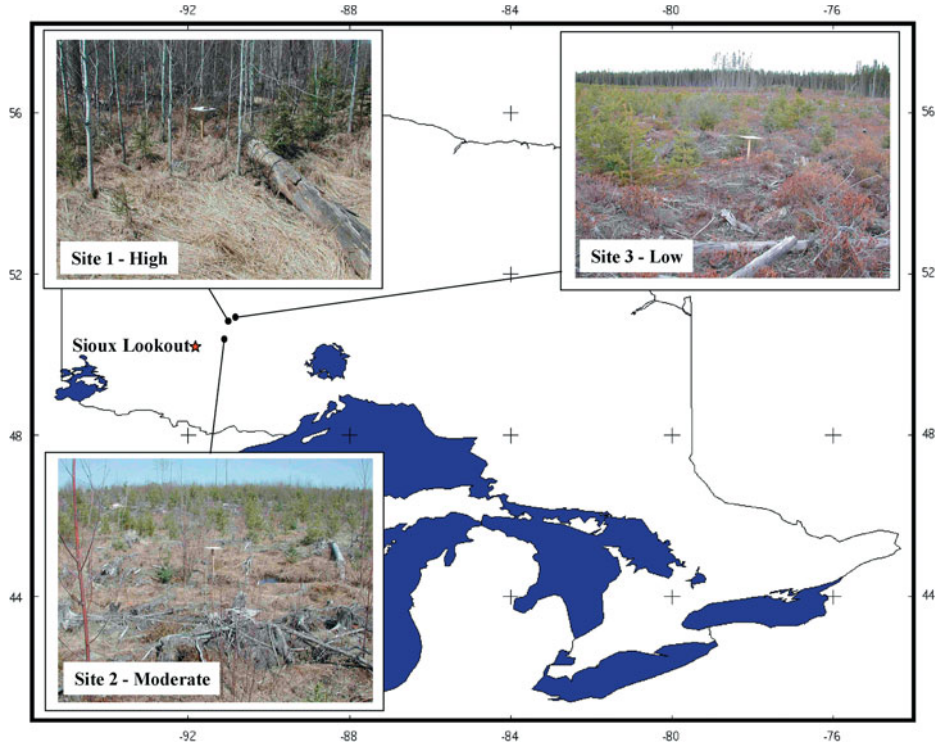

cies, indicative of rich soil with moderate moisture. Woody vegetation was abundant, with an approximate density of 8500 stems/ha for trees above 2 m in height. This layer was dominated by alder (*Alnus* spp.), but also contained aspen (*Populus tremuloides* Michx.). Both species considerably overtopped the crop trees. Grass was the most abundant herbaceous vegetation, occurring in patches where woody competition density was low. Topography was slightly sloping towards the southwest, with occasional small drainage channels. The size of the cut area was 11 ha, approximately 20% of which was sampled by the image transect.

The moderate site was planted with black spruce (*Picea mariana* (Mill.) BSP) in 1997, but in 2002 species composition was about 50% jack pine because of natural ingress. Total conifer density was 3172 stems/ha. The average crown diameter was 59.5 ± 33 cm, ranging from 6 to 135 cm. Average tree height was 110 cm. Competition consisted of pockets of high-density aspen and lower density white birch (*Betula papyrifera* Marsh.), with an overall density of 3400 stems/ha for trees above 2 m in height. Aspen tended to be considerably taller than birch, and both typically overtopped the spruce and pine. Herbaceous vegetation was dominated by grass and moss in moist valley areas. In higher areas, low woody shrubs were abundant. Topography was rolling, with associated wet areas in depressions and dry areas on higher ground. The size of the cut area was 20 ha, approximately 18% of which was sampled by the image transect.

The low site consisted of a 30:70 mixture of jack pine and black spruce, respectively. Spruce was planted in 1995 and was typically smaller than the natural ingress pine. Total conifer density was 4670 stems/ha. The average crown diameter was 55 ± 39 cm, ranging from 5 to 210 cm. The average tree height was 93 cm. The site had little to no competing vegetation, with no woody competitors greater than 2 m in height. Woody species included alder and willow (*Salix* spp.), while herbaceous competitors included Labrador tea (*Ledum groenlandicum* Oeder), mosses, lichens, and some sparse grasses. Topography was similar to the moderate site, with slightly rolling hills and associated wet and dry areas. The size of the cut area was 7 ha, approximately 34% of which was sampled by the image transect.

Field data

Sample plots were selected along a predetermined transect, with the objective of sampling the full range of conifer tree species, tree density, crown sizes, and woody competitor abundance on each of the sites. Circular plots with a radius of 3 m were used. For visual reference in subsequent imagery, plot centres were marked with a 40 cm × 40 cm white board, mounted on a 1.0 m tall stake. Each tree within the plot was assessed in relation to the plot centre by measuring the distance and direction from the centre to the tree. For each conifer tree in the plot, the species, stem height, stem diameter at ground level, and crown diameter (oriented north–south and east–west) were recorded. Position and tree measurement data were used to create a GIS layer for validation of automated detection–delineation results. The height of each woody stem within the plot was also recorded as a measure of competition.

Image data

Images were acquired under leaf-off conditions on 11 May 2002 between 1130 and 1500 local time, using a Duncantech MS3100 CIR digital camera with a 14 mm focal length Sigma aspherical lens. The camera was mounted in the front bay of a boom system attached to the undercarriage of a Bell Ranger helicopter. The camera uses beam-splitting optics to separate irradiance into three spectral bands that are imaged

Fig. 2. Flow chart showing stages involved in algorithm implementation.

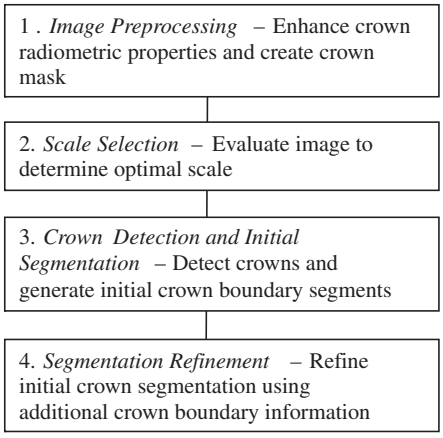

simultaneously by three charge-coupled devices (CCD). The spectral bandwidths are green (500–600 nm), red (600–700 nm), and near infrared (NIR, 700–900 nm). Each CCD comprises 1300 × 1000 photosites, which translates to 8-bit multispectral images of the same format. Shutter speed was set individually for each band to 1/200 s, 1/143 s, and 1/111 s, respectively, by viewing histograms of the target areas in flight. A flying height of 182 m was used to capture images with ~6 cm nominal ground pixel size and a spatial coverage of 83 m × 60 m. Flying speed varied between 2.2 and 3.3 m/s.

Tree detection–delineation algorithm

The detection–delineation algorithm developed for this study consists of the four stages shown in Fig. 2. The following sections describe in detail the specific processing carried out in each stage.

Image preprocessing

Image preprocessing is a flexible stage where the user selects the best spectral band and (or) enhances the image data to maximize crown distinction from background cover types and thus optimize algorithm performance. Common enhancements can include filtering to remove image noise and image transforms such as band ratios or the intensity or hue image from an IHS colour space transformation. The choice of enhancements depends on the imagery and requires some experimentation. For example, in Pouliot et al. (2002), a smoothed hue image was found to be the best enhancement for Kodak DCS 460 colour infrared imagery. In the present study, visual examination of the imagery revealed that the crown apexes and boundaries were most distinct in the NIR band and that image transformations and smoothing were not required.

Following initial band selection or enhancements, a conifer vegetation mask must be created to remove as much other vegetation (typically low-lying ground vegetation such as mosses) that is also green at this time of year. It can be created in a number of ways, but typically simple thresholding is sufficient or classification methods may be used if multispectral data are available. The conifer mask is used in all subsequent processing stages.

Fig. 3. The solid line is an example of a local maxima smoothing relation. The broken line indicates the visual rule used to determine the optimal Gaussian smoothing factor.

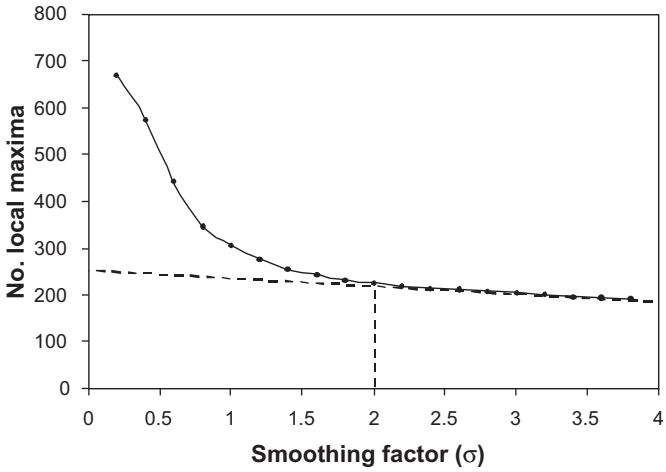

For this study, the original three spectral bands were classified into 100 clusters using the ISODATA algorithm (Jensen 1996) and aggregated into two final classes, conifers and nonconifers. This hyper-clustering approach was used because it allows for full control of the merging process and does not require the user to explicitly define class spectral properties, as is the case with supervised approaches. The binary mask created from the clustering process was dilated using a 3 × 3 structuring element to remove small holes in the mask and to ensure that the full extents of crowns were covered. The NIR image data under the mask were then extracted for the detection–delineation processing.

Scale selection

The scale at which imagery is acquired is often not the optimal scale for automated tree detection. At fine scales, small trees are more likely to be detected, but within-crown branching of large crowns can cause numerous false detection errors due to local maxima associated with within-crown branch clusters. At coarser scales, small trees may be missed or overlapping trees may be detected as a single crown. Thus, a scale optimization step is required to identify the scale that maximizes the detection of small trees while minimizing the detection of large crown branches and other image artifacts as individual crowns. Pouliot and King (2005) evaluated four approaches for optimal conifer detection in three different regenerating forest conditions using aerial photography and digital camera imagery. The best, and that used in this study, was adapted from a global approach presented in Culvenor (2000). In this approach the relation between scale simulated using a Gaussian filter and the number of local maxima identified (i.e., local maxima smoothing relation (LMSR)) was used to define the optimum scale. In examining this relation (Fig. 3), initial smoothing levels remove image noise and the number of local maxima drops rapidly with scale. This decrease then begins to slow down as noise is further removed, and within-crown branching starts to become the major source of additional local maxima. Further smoothing removes local maxima caused by within-crown branching, but also starts to remove small crowns, leading to omission error. Hence, there is a need to determine the point

that optimally balances the two error sources. An automated approach to selection of the optimal scale from the LMSR was suggested by Culvenor (2000) based on the maximum rate of change in the second derivative, but tests of this approach found it to be highly sensitive to local variations in the LMSR. Attempts to improve the automated selection procedure by applying smoothing algorithms (local averaging, Gaussian smoothing, and Lowess smoothing) to remove these variations revealed a strong dependence on the parameters selected. No logical criteria for parameter selection could be identified, making the selection an arbitrary trial and error process. Consequently, a more robust visual assessment procedure was adopted as described next.

The first step in visual assessment involved plotting the LMSR (Fig. 3). Then, the longest line that could be fit to the LMSR curve was determined, starting with the last point and moving towards the first point. This was defined as a linear fit where residuals were, in relative terms, small and equally distributed on either side of the line. In the final step, the point where this line and the curve started to diverge was determined. This point was taken as an indication of the optimal level of smoothing required. In this implementation, the LMSR was determined using a step size of 0.1σ within a range of 0–5. This scale selection approach is advantageous in that it does not require field data and provides information on the scaling properties of the crowns in the imagery that can be used to estimate a scale close to that of the optimum. Although repeatable (in tests of independent users), the main disadvantage is that it is subjective and requires users to calibrate amongst themselves. It is also limited by the degree to which commission and omission errors can be simultaneously minimized using a single global scale.

Crown detection and initial segmentation

Crown detection and initial segmentation were carried out using a watershed algorithm approach adapted from Persson et al. (2002), who applied it to lidar data in mature forest conditions. In this method, each pixel in the image is considered a seed and is forced to follow the local upward gradient until a local maximum point is reached. This seed pixel is then assigned to the cluster (or segment) for that local maximum position. The results of the algorithm produce an image with the same positions of local maxima as those obtained using a 3×3 local maximum filter. However, it also provides an initial segmentation of the crowns based on the cluster defined by pixels that climbed to a given local maximum point.

Segmentation refinement

The initial segmentation results from the gradient-following procedure are highly dependent on the quality of the crown mask created in stage 1, which in turn is dependent on the quality of the image data used and the image processing performed to create the mask. For example, brightness variations due to bidirectional and optical light fall-off effects can lead to the removal of crown pixels or addition of noncrown pixels, depending on the criteria used to separate crown and noncrown pixels. The purpose of the refinement step is to minimize this dependence by locally assessing the boundaries for each crown based on the initial gradient-following results. The refinement step was adapted from Pouliot et al. (2002). Starting at each local maximum, a user-specified number of transects around the candidate crown object are extended from the local maximum out to the local minimum boundary defined by the initial segmentation results, plus one additional pixel. The transect data are then extracted, and the maximum value in the first derivative is taken as the most suitable crown boundary position. In this study, crown boundaries were detected using the original unsmoothed imagery to avoid boundary distortion due to smoothing.

Detection–delineation evaluation

In mature forests, difficulties and costs associated with locating and measuring trees in the field have led to a large diversity of accuracy assessment procedures. However, in regenerating conditions it is easier to locate and measure trees in the field because of the reduced vertical structure. Thus, for validation, field-based measurement was conducted. Here, we present a standardized accuracy assessment procedure that can be used with field measurements to provide summary and indepth information regarding detection–delineation errors.

Visual assessment

One of the most effective means to acquire insight regarding processing results is visual evaluation. Prior to algorithm implementation, a set of four plots was selected that represented the unique characteristics of each transect. These plots included small trees, clustered groups of trees, and plots with high levels of woody stem competition. The detection–delineation results for these plots were examined to assess the general accuracy, identify errors, error commonalties, and error sources.

Quantitative assessment of detection results

Detection accuracy was quantitatively evaluated using a method adapted from Pitkanen (2001), where points from automated tree detection are assigned to ground-measured reference locations based on an iterative search distance algorithm. In the first iteration, all detected tree points from the automated processing within a given search distance of a reference tree location are found, the overlap between the segments for these points is calculated, and the largest overlap is assigned as a match to the reference point. Following this, the matched automated point and the reference point are removed from further consideration so that a given reference tree cannot be assigned to more than one detected tree. Overlap is taken as the average from both perspectives, that is, image to field segment and field to image segment. A minimum overlap threshold is also used to ensure that small overlapping segments are not considered. In subsequent iterations, a larger search distance is used, up to a maximum search distance of approximately half the size of the average tree crown size in the data set. In this study, the initial search distance was 0.1 m and the maximum search distance was 0.3 m, with the search distance increasing by 0.1 m for each iteration. The minimum overlap threshold was set at 20%. After the algorithm is complete, the reference trees not matched are taken as omission error, the detected trees not matched to a reference tree are taken as commission error, and the matched segments are considered correctly identified trees. The sizes of the test and reference segments associated with each match were also recorded so that the relation between detection accuracy and tree size could be evaluated. Detection results for minimum tree sizes of 30 and 60 cm

were evaluated. The numbers of omission, commission, and correctly identified trees are reported along with an accuracy index (Pouliot et al. 2002) calculated as

$$AI = [(n - o - c) / n] \times 100$$

where n is the actual number of trees in the study area and o and c are the numbers of omission and commission errors, respectively. With this index, both omission and commission errors are incorporated into a single summary value. Negative AI values are possible and occur when commission and omission errors are greater than the total number of trees counted in the field.

Empirically determined optimal scale

As the results of the detection algorithm were specifically for the image-based global smoothing factor selected using the procedure described previously, it was of interest to know what the accuracy would be if the optimal global smoothing factor was determined empirically through use of iterative accuracy assessment. To do this, each transect was smoothed using a Gaussian filter, with smoothing factors ranging from 1 to 3.5, in increments of 0.5σ. Local maxima were detected using the gradient following method, and accuracy results were compiled using the field data as described before. The optimal factor was taken as that which produced the highest AI.

Quantitative assessment of delineation results

Delineation accuracy was assessed by comparing the average crown dimensions for the matched trees using root mean square error (RMSE) and relative RMSE% calculated as

$$\text{RMSE\%} = \frac{\sqrt{\frac{1}{n}\sum (P_i - O_i)^2}}{\overline{O}} \times 100$$

where n is the number of observations, P_i is the predicted value from automated delineation, O_i is the observed value in the field, and $\overline{O}$ is the mean of the observed values. Mean absolute error (MAE) was also reported, as it is more robust to outliers, which can dramatically inflate RMSE values. Delineation error was evaluated first for all matched trees and second for those matched trees where only one automated segment was found to overlap a field reference ellipse by greater than 50%. This was done so that delineation results could be evaluated with minimal influence of detection error. Crown diameters for the automated delineations were measured in the same orientations as the field measurements and averaged. An automated method for crown diameter measurement was developed, which used the bounding rectangle to determine the crown centroid and then calculated the distance from the centroid to the polygon boundary.

Aggregated assessment of detection, delineation, and tree height

The results were also evaluated as aggregated estimates for the entire transect, as this reflects how they would most likely be used in regeneration assessment and management. Aggregate estimates of stem density and average crown diameter extracted from the detected–delineated crowns, as well as tree height modeled from crown diameter, were compared with field measurements to determine percent error. Height was estimated using the delineated crown diameter in a linear equation derived from the field data (Height = 1.34 × Crown_Diameter + 28, R^2 = 0.81, SE = 25 cm). Detection, delineation and tree height aggregate estimates were compared for all trees and for the 30- and 60-cm crown size thresholds.

Results

Visual assessment

Figure 4 shows the example plots that were selected for visual assessment. It should be noted that the blurry nature of the imagery was due to strong vibrations at the end of the boom that housed the camera. In all cases, it was apparent that crowns with strong brightness valleys were well delineated. Omission error occurred for small trees (A) and trees growing in close proximity or in large clumps (B). Commission error was less frequent in the example plots, with errors caused by low-lying ground vegetation (C) and within-crown brightness variability (D). Woody stem competition did not significantly hide trees from the sensor in this leaf-off imagery, but automated delineations do appear to be smaller than the field-measured ellipses for the plot shown in the bottom row of Fig. 4. Figure 5 shows sample areas for each transect at a scale suitable for a broad overview of the results.

Detection accuracy

The empirically determined optimal smoothing factor for each site was found to be 3σ, 2σ, and 1.5σ, giving AI values of 72.8%, 66.4%, and 44.9% for the high, moderate, and low transects, respectively (Table 1). These results are considered to be the best obtainable for this imagery and detection algorithm because the image scale has been optimized to achieve the highest agreement with the field data. In practice, however, field data would not typically be abundant enough to conduct such an analysis. Consequently, the scale selection step described previously was implemented as part of the overall detection–delineation algorithm, resulting in optimal smoothing factors of 2.4, 2, and 1.6 for the same transects. With these smoothing intensities, accuracies are within 3% of the empirically determined optima (Table 2, all trees), indicating that the visually based σ selection method performed well. The poorest results were observed for the low transect because of high omission error. Omission error for this transect was almost double that for the other two transects. Absolute commission error was largest for the moderate transect, but relative to the total number of field-counted trees, the high transect suffered the most from commission error.

To more fully understand the sources and magnitude of detection errors, omission and commission errors were visually evaluated and classified as to their most likely source. Figure 6 shows examples of errors of omission: a large crown overtops a smaller crown, hiding it from the sensor view (Fig. 6A), two proximal crowns result in a weak or nonexistent between-crown brightness valley (Fig. 6B), a very small isolated crown (15 cm diameter) with a signal too weak to be detected (Fig. 6C), a small crown (30 cm diameter) with a weak signal that is further reduced by the presence of competing vegetation (Fig. 6D). Errors of commission are also shown in Fig. 6: low-lying noncrop vegetation detected and

Fig. 4. Example results for selected plots. Yellow, automated crown delineations; green, field- located and field-measured crown ellipses. The rows represent site conditions as follows: row 1, plot showing typical conditions with a few large and small trees, some being in close proximity to one another; row 2, plot with mostly small trees, crown diameters from 10 to 40 cm; row 3, plot with a high degree of tree clustering; row 4, plot with a high degree of woody stem competition. Common detection errors are marked A, B, C, and D, as described in text.

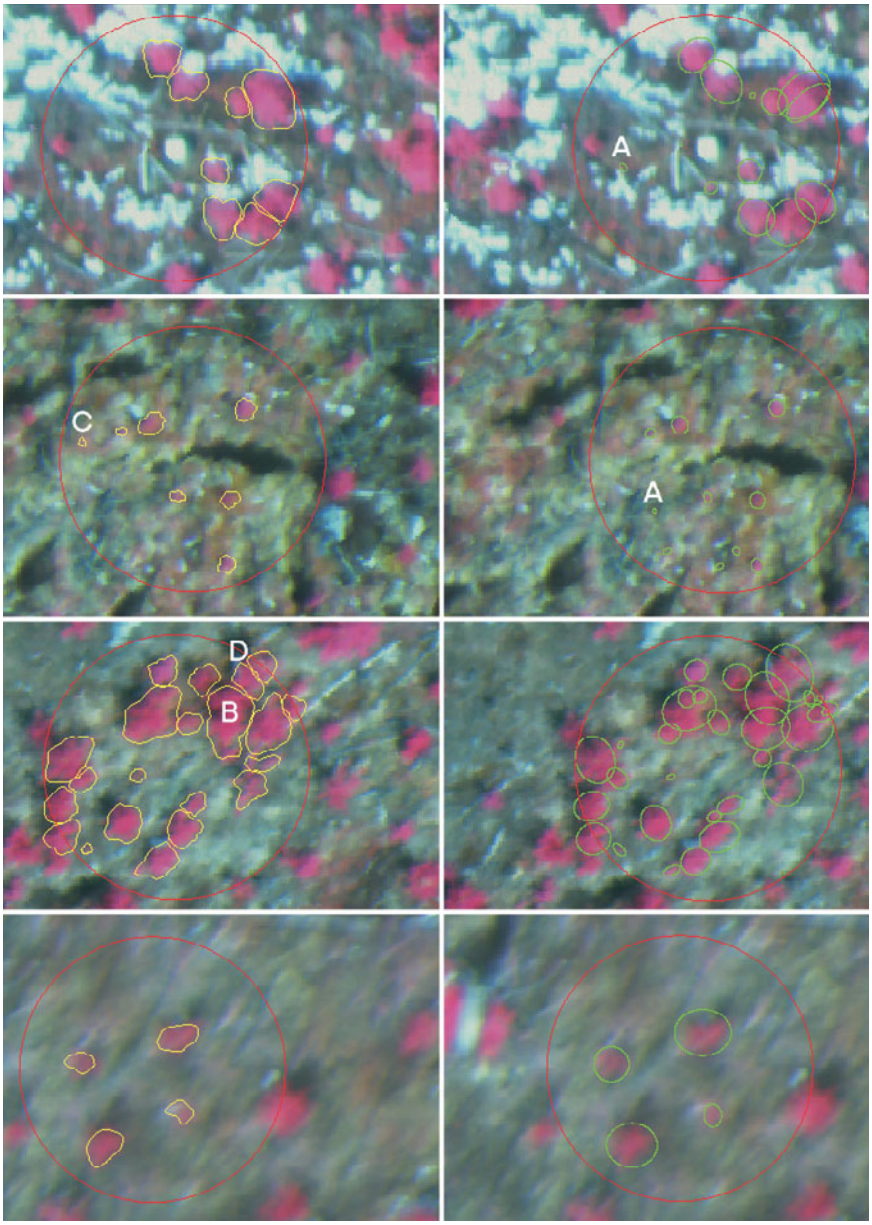

delineated as several tree crowns (Fig. 6E) and branch clusters in a crown detected and delineated as two crowns (Fig. 6F).

The largest source of detection omission error was the presence of tree crowns smaller than could be detected with this pixel size and the selected smoothing factors, but it was only greater than other error sources for the low transect (Table 3). Adjacent trees in close proximity were the second largest error source. Additional omission errors due to small trees being overtopped by larger conifers occurred in both the low and moderate transects. These transects are younger than the high transect, so sufficient competition between conifers and from overtopping woody vegetation has not yet resulted in mortality of these small trees. This has produced a more clumped spatial arrangement of conifers in the low and moderate sites than in the high site. The average diameter of omitted tree crowns was 32 ± 26 cm (mean ± SD). Woody competition did not significantly affect omission error.

Commission errors due to low-lying vegetation were greater than those due to within-crown branching. They typically consisted of small segments generated where a tree did not exist or, in the case of within-crown brightness variability, adjacent small and large segments generated for a single crown. The tree-matching algorithm used to evaluate accuracy takes the largest automated segment to represent the field-determined crown segment and the smaller automated

Fig. 5. Example overview images of detection–delineation results for the three transects. Top, low; middle, moderate; bottom, high.

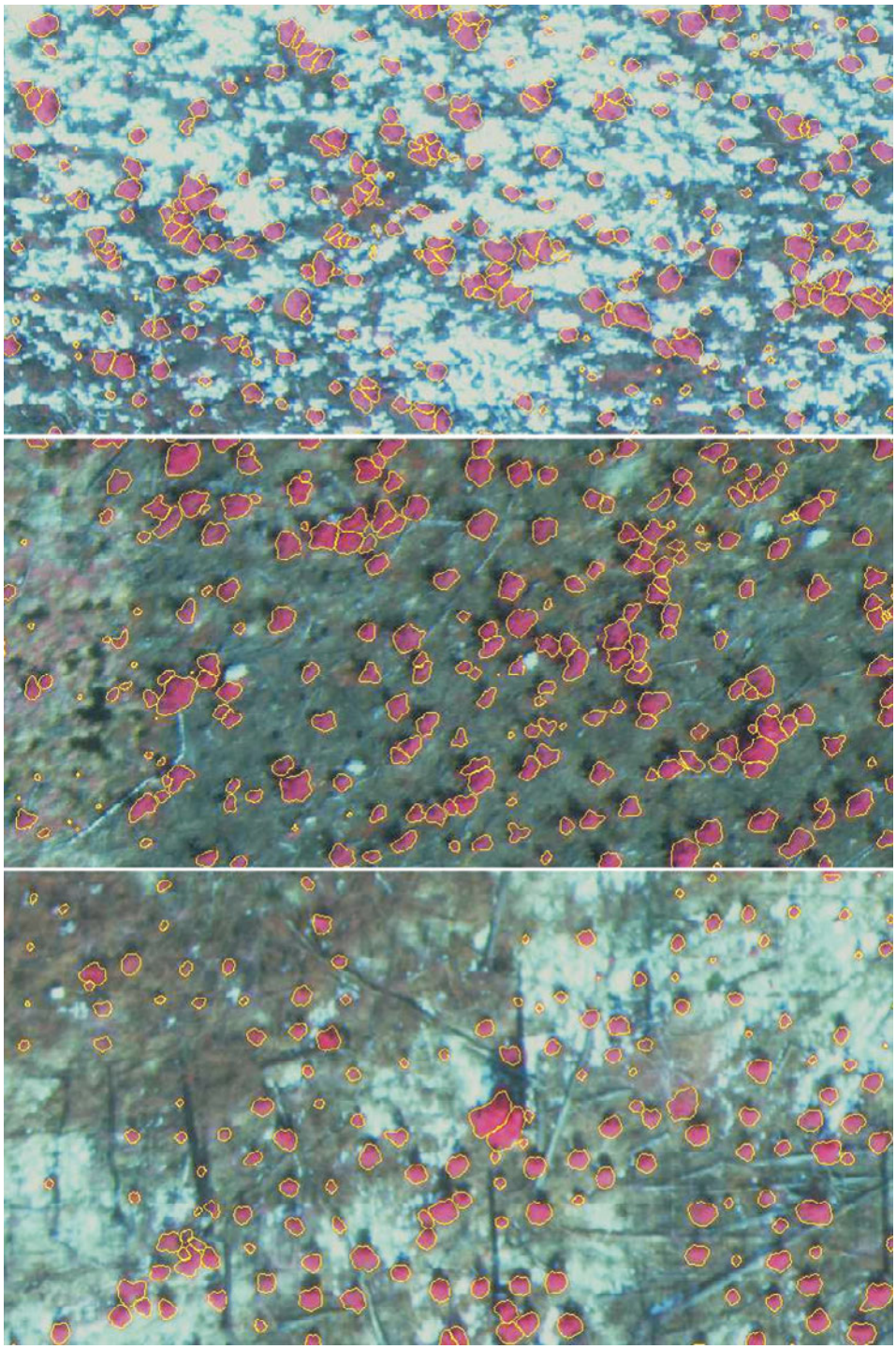

segments are taken as commission errors. The average diameter of commission error segments was 50 ± 33 cm.

Because detection errors were caused by small trees being missed or by the generation of small but false segments in the processing results, substantial improvement is possible by thresholding the crown sizes used for validation. Increasing the minimum crown size to 30 cm dramatically improved results for all three transects, with the greatest increase in AI (22%) occurring for the low transect (Table 2). At this size threshold, two of the three sites have AI >80%. Increasing the minimum crown size to 60 cm again increased accuracy, but at a slower rate as the accuracies approached 100%.

Delineation accuracy

For all matched crowns, the MAE error for delineation ranges from 15% to 23% (Table 4). RMSE% values are higher (22%–35%), showing that RMSE% is more affected by extreme values in the data. Results for crowns matched as one automated segment to one field reference ellipse (i.e., 1:1) show considerable improvement, with MAE% values

Table 1. Detection accuracy with increasing Gaussian smoothing intensity for plots in low, moderate, and high transects; values are tree counts unless specified otherwise.

Plot	Smoothing factor (σ)	Omission	Commission	Correct	Correct %	AI %
Low	1.0	113	66	143	55.9	30.1
Low	1.5	125	16	129	50.4	44.9
Low	2.0	135	9	121	47.3	43.8
Low	2.5	143	5	113	44.1	42.2
Low	3.0	151	5	105	41.0	39.1
Low	3.5	152	5	104	40.6	38.7
Moderate	1.0	43	87	222	83.8	50.9
Moderate	1.5	55	36	210	79.2	65.7
Moderate	2.0	64	25	201	75.8	66.4
Moderate	2.5	71	21	194	73.2	65.3
Moderate	3.0	75	19	190	71.7	64.5
Moderate	3.5	78	19	187	70.6	63.4
High	1.0	11	46	103	90.4	50
High	1.5	14	33	100	87.7	58.8
High	2.0	14	19	100	87.7	71.1
High	2.5	16	18	98	86.0	70.2
High	3.0	16	15	98	86.0	72.8
High	3.5	17	15	97	85.1	71.9

Note: AI, accuracy index.

Table 2. Detection accuracy for all trees and for trees with crown diameters greater than 30 and 60 cm; values are tree counts unless specified otherwise.

Transect	Min. crown size	Omission	Commission	Correct	Total	Correct %	AI %
Low	All	125	10	129	256	50.4	47.3
Low	>30 cm	44	7	124	168	73.8	69.6
Low	>60 cm	16	2	78	94	83.0	80.9
Moderate	All	64	25	201	265	75.8	66.4
Moderate	>30 cm	22	13	186	208	89.4	83.2
Moderate	>60 cm	7	4	118	125	94.4	91.2
High	All	15	19	99	114	86.8	70.2
High	>30 cm	7	7	97	104	93.3	86.7
High	>60 cm	2	5	67	69	96.7	90.0

Note: AI, accuracy index.

Fig. 6. Examples of detection error sources. Green segments are field-measured reference ellipses; yellow segments are automated delineation results. Figures 6A–6D show omission errors, and Figs. 6E–6F show commission errors, as described in the text.

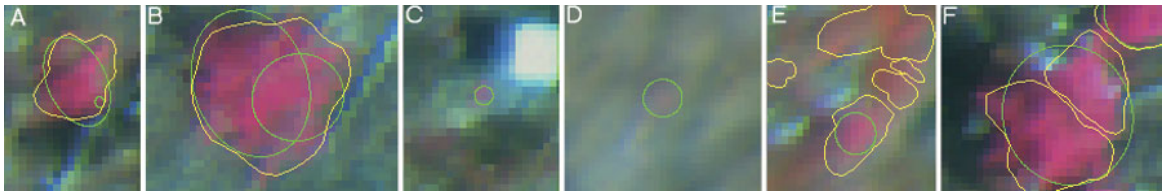

ranging from 13% to 17%. For these trees, strong linear relations were found, with R^2 values ranging from 0.76 to 0.87 and slopes close to 1, but with varying magnitude and direction of offsets (Fig. 7). Larger crowns in the imagery tended to be underestimated by the delineation algorithm. This error is more prevalent for the high transect and explains why it had the poorest delineation results. For the low transect there was a slight overestimation of small crowns less than about 50 cm in diameter.

The average plot error, in terms of the difference between image- and field-measured crown diameter, showed a weak relation with the number of competing woody stems within the plot (Fig. 8). The relation was stronger when only woody stems above 2.5 m in height were counted. This was due to the effect of the increased overtopping of larger trees, which tended to obscure the conifer crown boundaries to a greater degree. Although there does appear to be a relation, it does not consistently produce errors that are larger than those caused by noncompetition factors (i.e., spread of errors where little or no competition was present).

Table 3. Counts of detection error category and source.

	Omission error				Commission error	
Transect	Adjacent overtopped tree	Adjacent trees in close proximity	Small tree	Small tree with competition	Branch pattern	Low ground vegetation
Low	7	35	83	0	6	4
Moderate	16	23	23	5	4	21
High	0	5	5	5	7	12
Total	23	63	111	10	17	37

Table 4. Summary statistics for delineation accuracy.

Transect	R^2	Slope	Offset	MAE (cm)	MAE %	RMSE (cm)	RMSE%
Low	0.64	1.1	–9.5	16.1	20	22.7	28.8
Low (1:1)	0.73	1.12	–7.8	10.5	14.15	14.5	20.6
Moderate	0.76	1	2.1	10.5	15	15.1	21.7
Moderate (1:1)	0.82	1.01	0.05	9	13.3	12.8	18.9
High	0.6	1.1	–1.6	18.7	22.7	28.7	34.9
High (1:1)	0.75	1.05	1.07	13.2	17.1	17.6	22.7

Note: MAE, mean absolute error; RMSE, root mean square error.

Fig. 7. Scatterplots of field-measured versus image-measured average crown diameter for trees matched as one automated segment to one reference ellipse (i.e., 1:1). Solid line represents $y = x$.

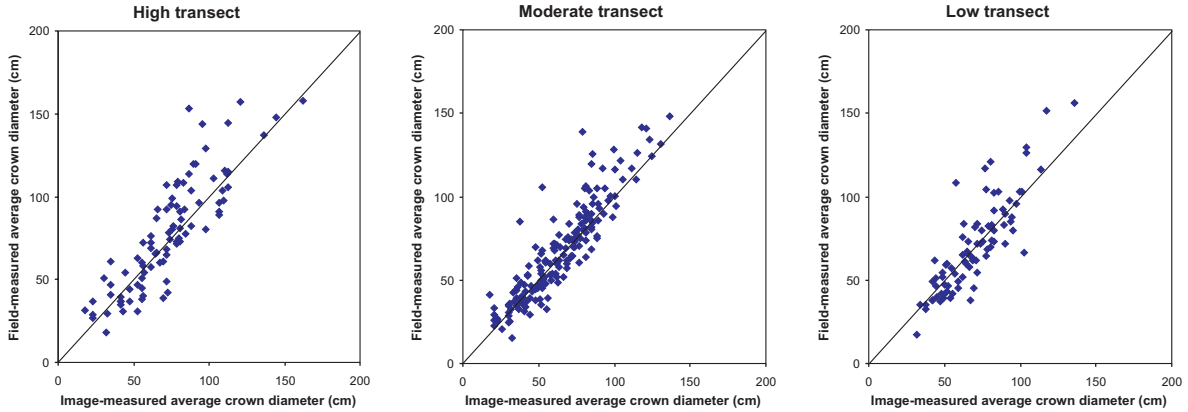

Aggregated detection–delineation errors

In aggregation of the results for each transect, errors were lower than the individual tree comparisons (Table 5). The best results were found for the 30 cm crown size threshold. Increasing the threshold to 60 cm improved detection, but errors for crown diameter and tree height increased because of the greater error in delineation of larger trees. For crown diameter and height estimates, exclusion of trees less than 30 cm produced very high accuracy for the low transect and good accuracy for the others. As these results reveal, the improvements due to aggregation are strongly influenced by the bias in the individual estimates. This is evident for the crown diameter comparisons, which, on an individual basis, resulted in larger crown sizes being underestimated, leading to larger error for aggregated comparisons with larger crown sizes.

Discussion

Detection accuracy

On an individual-tree basis, moderate accuracies for detection of 6–300 cm tall conifers (AI = 48%–70%) were produced using the algorithm implemented on 6 cm pixel size digital camera imagery. Application of minimum crown diameter thresholds of 30 and 60 cm improved detection accuracies to 70%–87% and 81%–91%, respectively. This was because most errors of omission and commission were linked to small trees or low-lying non-tree vegetation. Depending on management and sampling objectives, the omission of such small trees may be inconsequential. This tree size influence was also seen in the aggregated transect-level comparison, where accuracies were significantly better for crowns larger than 30 cm. The low-competition transect, which had many small crowns that could not be detected, produced the greatest improvement in accuracy when the small trees were excluded.

The high omission error observed in the low transect was due to two factors. First, the crown size distribution of the low transect was skewed towards smaller crowns, of which there were many. Second, the preprocessing step used to extract the crowns (unsupervised cluster labeling) was biased towards missing many of these small crowns. The bias resulted from the abundance of low-lying vegetation at this

Fig. 8. Scatterplots showing the difference between image- and field-measured mean plot crown diameter and the stem density of woody competition.

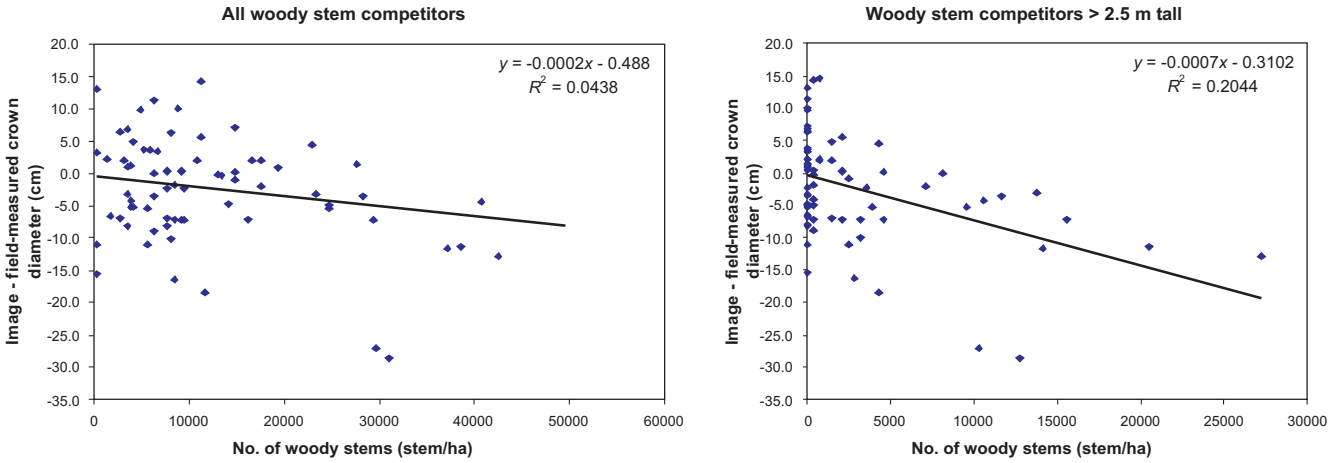

Table 5. Transect mean and percent difference measures between image- and field-measured tree density, crown diameter, and tree height.

		Tree density (stems/ha)			Crown diameter (cm)			Tree height (cm)		
Transect	Min. crown size	Image	Field	% error	Image	Field	% error	Image	Field	% error
Low	All	2459.3	4529	–45.7	75.4	55	37.1	127.7	93	37.3
Low	>30	2317.8	2972	–22.0	75.4	76.1	–0.9	127.7	125.8	1.5
Low	>60	1415.4	1663	–14.9	88.3	95.6	–7.6	145.3	151.8	–4.3
Moderate	All	3998.6	4689	–14.7	63.5	59.5	6.7	112.4	110	2.2
Moderate	>30	3520.9	3680	–4.3	67.7	71.1	–4.8	117.9	128	–7.9
Moderate	>60	2158.5	2212	–2.4	83.5	88.4	–5.5	150.6	140	7.6
High	All	2087.8	2017	3.5	71.2	77	–7.5	123.4	138	–10.6
High	>30	1831.2	1833	0.1	76.8	83.3	–7.8	131	147	–10.9
High	>60	1261.5	1221	3.3	89.4	102	–12.4	148	170	–12.9

site, particularly mosses, which could not be adequately separated from the small crowns in the creation of the crown mask. Thus, omission error due to small crowns was preferred over commission error due to low-lying vegetation in this transect. This same bias was applied when extracting crown pixels from the other two transects, but the resulting error was not as extreme because the moderate and high transects did not have as many small crowns.

Additional means to improve detection of small trees include improvement of image quality and modification of data acquisition timing, data types, and image processing. The quality of imagery acquired for this study was poor relative to what was expected for 6-cm pixel size. Although the flight speed was low, the strong boom vibration caused significant image motion blurring. Either faster shutter speeds and (or) a more vibration isolated mount would reduce these effects and provide for more precise tree detection and crown boundary delineation. In terms of image timing, true leaf-off imaging cannot be considered a viable solution, as many mosses maintain their greenness throughout the year and many grasses were green within a few days of snowmelt. Such a narrow time period for image acquisition is too limiting for operational applications. Instead, data could be acquired in winter; however, snow depth would have to be monitored and acquisition would have to be carried out when snow has melted off crowns. If other data types can be considered, combined use of digital camera imagery and lidar would be advantageous, although costs associated with lidar systems can be high. Leckie et al. (2003) compared detection–delineation results for both sensors in mature forest conditions and found that lidar data were particularly useful in more open forest conditions, because a simple height threshold could be applied to remove false detection due to what was considered to be low-lying vegetation. Implementing an improved classification methodology is a potentially low-cost alternative. Object-based classification, such as that available with the commercial package eCognition, may be used to separate low-lying vegetation from coniferous crowns. The advantage is that the spectral responses of objects such as small crowns and low-lying vegetation that are generated by such a region-growing procedure are likely to be more distinct than the individual pixels contained in each object.

Omission errors caused by small trees and trees in close proximity as well as commission errors due to oversegmentation of trees with strong branching patterns are errors related to image scale. At scales with more detail there is an increased probability of correctly detecting small trees and trees in close proximity because the local valley brightness gradients used to separate crowns are more distinct. However, for large crowns, fine scales tend to retain distinct

brightness valleys due to branches rather than crown boundaries, leading to false crown detection–delineation. Ideally, the appropriate scale for detecting a particular tree should be defined by the image characteristics in the local vicinity of the crown. Unfortunately, this is not a simple task. Pouliot and King (2005) found that for conditions with variable tree size and spacing, the best detection results were obtained using a locally determined scale instead of a global scale. However, the local approach proved to be highly parameter intensive and therefore was not considered operationally useful, nor suitable for the present study. Further research in scaling for optimal feature extraction and other optimal detection approaches is needed to overcome this general limitation of segmentation methods.

Delineation accuracy

In previous research using a more simplified algorithm under controlled tree spacing and competition conditions, Pouliot et al. (2002) found individual tree delineation accuracies for crowns detected as 1:1 to have RMSE% = 17.9% for 5 cm pixel spacing imagery. In this study, under uncontrolled operational conditions with a more advanced algorithm, RMSE% was 19%–23%. As identified in this study, Pouliot et al. (2002) also found that the large crowns were underestimated by the detection–delineation processing. For spatially aggregated results, Gougeon and Leckie (1999) compared average crown diameters for entire stands and found errors ranging from 7% to 9%. In Pouliot et al. (2002) whole-plot error was 3%. In this study, whole-transect error ranged from 7% to 37% for all trees and from 1% to 8% when only trees with a crown diameter greater than 30 cm were considered. The major difference between these studies, apart from the algorithms and image pixel sizes used, was the size and spacing variability of the trees, with much less variability in the studies presented by Gougeon and Leckie (1999) and Pouliot et al. (2002). In mature forests, Brandtberg and Walter (1998) did not find a significant relation between field- and image-measured crown diameters. Persson et al. (2002) reported an RMSE of 0.61 m using lidar data, but the average crown diameter was not reported and could only be inferred from graphs given in their study. Assuming an average crown diameter of 5 m, their results are quite good with an RMSE of ~12%. The field and image measures were also linearly related (r^2 = 0.76) and, like the results presented here, tended to slightly underestimate larger crowns.

Delineation error is heavily tied to detection error because of the effects of commission error for large crowns reducing the crown size estimates. Thus, the improvements identified for detection will improve the delineation results. Further improvement in delineation accuracy is also possible with subpixel processing. For the data used in this study, the 6 cm pixel size and selected smoothing factors could result in diameter estimate errors of approximately 1–6 cm depending on how the 6-cm grid of the acquired image data overlaid the tree crowns. For example, a mixed pixel with an area of 55% conifer and 45% soil would be seen as a crown pixel. If this pixel is used in the crown diameter estimate it would cause an over estimation of the crown diameter by ~3 cm because of the mixed pixel effect. Thus, if two of these pixels are included in the diameter estimate, a maximum error of ~6 cm could result. This suggests possible errors of up to 9%, considering the average crown size for transects in this study was 65 cm. Another important source of error was the field measurements, which showed the average MAE to be 5 cm based on a remeasurement of 30 trees. Thus, an additional 8% error was possible.

Effect of competition

The effect of adjacent and overtopping woody stem vegetation on conifer detection–delineation accuracy was small relative to other sources. Small crowns in plots with or without high competition were difficult to accurately detect, and there were insufficient data on small crowns in high-competition areas to conclusively assess competition effects. Larger crowns (i.e., >30 cm) were detected successfully with competition present. Delineation error was more clearly affected by the presence of competing vegetation and tended to generally reduce crown size estimates. However, in many cases it appeared that competition was a less important factor for delineation error than other error sources such as image scale and spatial arrangement of trees. The use of plot averages to represent competition intensity rather than individual measurements was a significant limitation of this analysis. These measurements were made on a plot level to satisfy several analysis objectives. Individual measurements would have been preferred, as there was considerable variability in tree size, spacing, and spatial arrangement of both conifers and woody competition stems within the plots. The presence of this variability reduces the utility of the mean plot measures to be used for comparisons among plots. Despite these limitations, the results do suggest that competing vegetation is potentially less important than other sources of error.

Operational considerations

Image data quality plays an important role in both detection and delineation. Factors such as sensor view angle, sun elevation, and topography have a significant effect on the radiometric and geometric properties of the tree crowns. Using simulated imagery of mature *Eucalyptus* forests, Culvenor (2000) showed that detection accuracy performance was best with small off-nadir view angles (i.e., <15°) using backscattered as opposed to forward-scattered image data and higher solar zenith angles. To reduce optical- and illumination-view angle (i.e., bidirectional) effects, imagery with narrow view angles can be acquired with a high degree of overlap and used in subsequent mosaic generation. The effect of topography has not been widely researched. Culvenor et al. (2000) found that the effects of topography depended on the incident radiation relative to the topographic slope and aspect. At the tree level, differences in illumination due to topography cause differences in mutual shading of crowns and the brightness response of the background. At a coarser scale, topography produces shaded and sunlit slopes that make it difficult to effectively extract an accurate crown mask. More research is needed to develop appropriate means to reduce both crown-level and terrain-level topographic brightness effects on detection–delineation accuracy. Topography also affects pixel size, which in turn can impact crown size estimates, but this effect could be minimized through orthorectification if a suitable digital elevation model can be derived.

With the image pixel size used in this study, the proposed methodology would most likely be used in a strip-sampling approach to acquire greater sample coverage than could be obtained through field surveys. Such a methodology provides a potentially lower cost means to increase sample coverage, access remote areas, and retain a permanent visual record of the site conditions. An indepth economic analysis is beyond the scope of this study, but eventually will have to be performed. Here the major cost was the use of the helicopter, billed at CAN$1200/h. Alternatively, fixed-wing aircraft could be used at lower cost, but a camera with capability for higher shutter speeds than those used in this study would be required because of the associated increased flying speed. In comparison to field surveys, this approach provides the means to dramatically increase sample coverage, which cannot be achieved through field sampling. Further, the collected data can be used in other applications in addition to regeneration inventory.

Conclusion

An automated tree detection–delineation algorithm developed for monitoring regenerating forest conditions was presented and evaluated. Detection accuracy was moderate when all trees were considered and improved significantly to acceptable levels when very small trees (crown size <30 cm) were excluded. The most significant factors found to affect detection were small trees, trees close together such that little or no distinct brightness valley was evident between them, and the presence of low-lying vegetation. Crown delineation MAE was <23% of field-measured crown diameter, and large tree crown diameters were often underestimated. The presence of competing woody vegetation did not have a strong influence on detection and had only a small effect on delineation accuracy, with increasing competition reducing crown size estimates slightly. If applied to narrow view angle imagery with a small enough pixel size relative to the crown sizes that are required to be detected and measured, this algorithm could complement or replace field-based regeneration surveys.

Acknowledgements

This research was funded by grants to D. King and scholarships to D. Pouliot from the Natural Sciences and Engineering Research Council of Canada (NSERC). The contributions from Wayne Bell, Mark Lindsay, Duncantech Ltd., Wiskair Ltd., and Buchanan Forest Products Ltd. to this research are also much appreciated.

References

Brandtberg, T. 1999. Algorithms for structure- and contour-based tree species classification using digital image analysis. *In* Proceedings of the International Forum on Automated Interpretation of High Spatial Resolution Digital Imagery for Forestry, Victoria, B.C., 10–12 February 1998. Canadian Forest Service, Natural Resources Canada, Victoria, B.C. pp. 199–205.

Brandtberg, T., and Walter, F. 1998. Automated delineation of individual tree crowns in high spatial resolution aerial images by multiple-scale analysis. Mach. Vision Appl. **11**: 64–73.

Culvenor, D.S. 2000. Development of a tree delineation algorithm for application to high spatial resolution digital imagery of Australian native forest. Ph.D. thesis, University of Melbourne, Australia.

Culvenor, D.S. 2003. Extracting individual tree information : a survey of techniques for high spatial resolution imagery. *In* Remote sensing of forest environments: concepts and case studies. *Edited by* M.A. Wulder and S.E. Franklin. Kluwer Academic Publishers, Boston, Mass. pp. 255–277.

Dralle, K., and Rudemo, M. 1996. Stem number estimation by kernel smoothing in aerial photos. Can. J. For. Res. **26**: 1228–1236.

Erikson, M. 2003. Segmentation of individual tree crowns in colour aerial photographs using region growing supported by fuzzy rules. Can. J. For. Res. **33**: 1557–1563.

Erikson, M. 2004. Species classification of individually segmented tree crowns in high-resolution aerial images using radiometric and morphologic image measures. Remote Sens. Environ. **91**: 469–477.

Goba, N., Pala, S., and Narraway, J. 1982. An instruction manual on the assessment of regeneration success by aerial survey. Ontario Ministry of Natural Resources publication, Toronto, Ont.

Gougeon, F.A. 1995. A crown-following approach to the automatic delineation of individual tree crowns in high spatial resolution images. Can. J. Remote Sens. **21**: 274–288.

Gougeon, F.A., and Leckie, D.G. 1999. Forest regeneration: individual tree crown detection techniques for density and stocking assessments. *In* Proceedings of the International Forum on Automated Interpretation of High Spatial Resolution Digital Imagery for Forestry, Victoria, B.C., 10–12 February 1998. Canadian Forest Service, Natural Resources Canada, Victoria, B.C. pp. 169–177.

Haddow, K.A., King, D.J., Pouliot, D.A., Pitt, D.G., and Bell, F.W. 2000. Early regeneration conifer identification and competition cover assessment using airborne digital camera imagery. For. Chron. **76**: 915–928.

Hall, R.J. 1984. Use of large-scale aerial photographs in regeneration assessments. Can. For. Serv. North. For. Res. Cent. Inf. Rep. NOR-X-264.

Hall, R.J., and Aldred, A.H. 1992. Forest regeneration appraisal with large-scale aerial photographs. For. Chron. **68**: 142–150.

Hayward, C., and Slaymaker, D. 2001. Estimating the significant above ground biomass of Amazonian Rain Forest using low altitude aerial videography. *In* Proceedings 18th Biennial Workshop on Color Photography and Videography in Resource Assessment, Amherst, Massachusetts, 16–18 May 2001 [CD-ROM]. American Society of Photogrammetric and Remote Sensing, Bethesda, Md.

Holmgren, J., and Persson, A. 2003. Identifying species of individual trees using airborne laser scanner. Remote Sens. Environ. **90**: 415–423.

Jensen, J.R. 1996. Introductory digital image processing: a remote sensing perspective. Prentice Hall, Upper Saddle River, N.J.

King, D.J. 2000. Airborne remote sensing in forestry: sensors, analysis and applications. For. Chron. **76**: 859–876.

Leckie, D.G., Gougeon, F.A., Hill, D., Quinn, R., Armstrong, L., and Shreenan, R. 2003. Combined high-density lidar and multispectral imagery for individual tree crown analysis. Can. J. Remote Sens. **29**: 633–649.

Leckie, D.G., Jay, C., Gougeon, F.A., Sturrock, R.N., and Paradine, D. 2004. Detection and assessment of trees with *Phellinus weirii* (laminated root rot) using high resolution multi-spectral imagery. Int. J. Remote Sens. **25**: 793–818.

Leckie, D.G., Gougeon, F.A., Tinis, S., Nelson, T., Burnett, C., and Paradine, D. 2005. Automated tree recognition in old-growth co-

nifer stands with high-resolution digital imagery. Remote Sens. Environ. **94**: 311–326.

Niemann, K.O., Adams, S., and Hay, G. 1999. Automated tree crown identification using digital orthophoto mosaics. *In* Proceedings of the International Forum on Automated Interpretation of High Spatial Resolution Digital Imagery for Forestry, Victoria, B.C., 10–12 February 1998. Canadian Forest Service, Natural Resources Canada, Victoria, B.C. pp. 105–108.

Persson, A., Holmgren, J., and Soderman, U. 2002. Detecting and measuring individual trees using an airborne laser scanner. Photogramm. Eng. Remote Sens. **68**: 925–932.

Pinz, A. 1999. Tree isolation and species classification. *In* Proceedings of the International Forum on Automated Interpretation of High Spatial Resolution Digital Imagery for Forestry, Victoria, B.C., 10–12 February 1998. Canadian Forest Service, Natural Resources Canada, Victoria, B.C. pp. 127–139.

Pitkanen, J. 2001. Individual tree detection in digital aerial images by combining locally adaptive binarization and local maxima methods. Can. J. For. Res. **31**: 832–844.

Pitt, D.G., and Glover, G.R. 1993. Large-scale 35-mm aerial photographs for assessment of vegetation-management research plots in Eastern Canada. Can. J. For. Res. **23**: 2159–2169.

Pitt, D.G., Wagner, R.G., Hall, R.J., King, D.J., Leckie, D.G., and Runesson, U. 1997. Use of remote sensing for forest vegetation management: a problem analysis. For. Chron. **73**: 459–478.

Pitt, D.G., Runesson, U., and Bell, F.W. 2000. Application of large- and medium-scale aerial photographs to forest vegetation management: a case study. For. Chron. **76**: 903–913.

Pollock, R. 1999. Individual tree recognition based on a synthetic tree crown image model. A spatial clustering approach to automated tree crown delineation. *In* Proceedings of the International Forum on Automated Interpretation of High Spatial Resolution Digital Imagery for Forestry, Victoria, B.C., 10–12 February 1998. Canadian Forest Service, Natural Resources Canada, Victoria, B.C. pp. 25–34.

Pouliot, D.A., and King, D.J. 2005. Approaches for optimal automated individual tree crown detection in regenerating coniferous forests. Can. J. Remote Sens. **31**: 255–267.

Pouliot, D.A., King, D.J., Bell, F.W., and Pitt, D.G. 2002. Automated tree crown detection and delineation in high-resolution digital camera imagery of coniferous forest regeneration. Remote Sens. Environ. **82**: 322–334.

Walsworth, N.A., and King, D.J. 1999. Image modeling of forest changes associated with acid mine drainage. Comput. Geosci. **25**: 567–580.

Wulder, M., Niemann, K.O., and Goodenough, D.G. 2000. Local maximum filtering for the extraction of tree locations and basal area from high spatial resolution imagery. Remote Sens. Environ. **73**: 103–114.